

# Deep-sea coral evidence for lower Southern Ocean surface nitrate concentrations during the last ice age

Xingchen Tony Wang<sup>a,b,1,2</sup>, Daniel M. Sigman<sup>a</sup>, Maria G. Prokopenko<sup>c</sup>, Jess F. Adkins<sup>d</sup>, Laura F. Robinson<sup>e</sup>, Sophia K. Hines<sup>d</sup>, Junyi Chai<sup>f</sup>, Anja S. Studer<sup>b</sup>, Alfredo Martínez-García<sup>b</sup>, Tianyu Chen<sup>e</sup>, and Gerald H. Haug<sup>b,g</sup>

<sup>a</sup>Department of Geosciences, Princeton University, Princeton, NJ 08544; <sup>b</sup>Climate Geochemistry Department, Max Planck Institute for Chemistry, 55128 Mainz, Germany; <sup>c</sup>Department of Geology, Pomona College, Claremont, CA 91711; <sup>d</sup>Division of Geological and Planetary Sciences, California Institute of Technology, Pasadena, CA 91125; <sup>e</sup>Bristol Isotope Group, School of Earth Sciences, University of Bristol, Bristol BS8 1RJ, United Kingdom; <sup>f</sup>Atmospheric and Oceanic Sciences Program, Princeton University, NJ 08544; and <sup>g</sup>Geological Institute, ETH Zürich, 8092 Zurich, Switzerland

Edited by Mark H. Thieme, University of California, San Diego, La Jolla, CA, and approved February 15, 2017 (received for review September 20, 2016)

The Southern Ocean regulates the ocean's biological sequestration of CO<sub>2</sub> and is widely suspected to underpin much of the ice age decline in atmospheric CO<sub>2</sub> concentration, but the specific changes in the region are debated. Although more complete drawdown of surface nutrients by phytoplankton during the ice ages is supported by some sediment core-based measurements, the use of different proxies in different regions has precluded a unified view of Southern Ocean biogeochemical change. Here, we report measurements of the <sup>15</sup>N/<sup>14</sup>N of fossil-bound organic matter in the stony deep-sea coral *Desmophyllum dianthus*, a tool for reconstructing surface ocean nutrient conditions. The central robust observation is of higher <sup>15</sup>N/<sup>14</sup>N across the Southern Ocean during the Last Glacial Maximum (LGM), 18–25 thousand years ago. These data suggest a reduced summer surface nitrate concentration in both the Antarctic and Subantarctic Zones during the LGM, with little surface nitrate transport between them. After the ice age, the increase in Antarctic surface nitrate occurred through the deglaciation and continued in the Holocene. The rise in Subantarctic surface nitrate appears to have had both early deglacial and late deglacial/Holocene components, preliminarily attributed to the end of Subantarctic iron fertilization and increasing nitrate input from the surface Antarctic Zone, respectively.

Southern Ocean | nutrient consumption | atmospheric CO<sub>2</sub> | ice ages

Phytoplankton grow in the sunlit surface waters of the ocean, transforming carbon dioxide (CO<sub>2</sub>) into organic carbon, and the portion of this organic carbon that sinks out of the surface ocean (“export production”) effectively transfers CO<sub>2</sub> from the surface waters and the overlying atmosphere into the dark, deep ocean. In parallel with carbon, the nutrients required in large quantities by all phytoplankton (the “major nutrients” nitrogen, N, and phosphorus, P) are also exported out of the surface ocean and stored in the deep ocean. The “efficiency” of the biological pump is a global measure of the degree to which marine organisms exploit the major nutrients in the ocean to produce sinking organic matter. A higher efficiency of the biological pump stores more CO<sub>2</sub> in the deep ocean, lowering the partial pressure of CO<sub>2</sub> (pCO<sub>2</sub>) in the atmosphere (1).

In today's Southern Ocean, due to limitation by light and the trace nutrient iron (2, 3), phytoplankton consume only a small fraction of the available N and P, lowering the efficiency of the global ocean's biological pump, which is manifested regionally as the leakage of deeply stored CO<sub>2</sub> through the Southern Ocean surface and back to the atmosphere (4). Changes in the degree of N and P consumption in the Southern Ocean may have played a role in past changes in atmospheric pCO<sub>2</sub>, especially on glacial–interglacial timescales (5). Since the discovery that the ice age pCO<sub>2</sub> was approximately one-third lower than the preindustrial pCO<sub>2</sub> (6), research has been ongoing to reconstruct the biogeochemistry of the Southern Ocean over glacial cycles (5, 7, 8). Relative to interglacials such as the Holocene, reconstructed ice age export production was higher in the Subantarctic Zone (SAZ) but lower in the Antarctic Zone (AZ) (5, 9). Understanding this pattern requires additional biogeochemical information. A complementary constraint,

which speaks more directly to air–sea CO<sub>2</sub> exchange, is how the degree of nutrient consumption varied in each of these two zones of the Southern Ocean.

The nitrogen isotopic composition of organic matter has the potential to record the degree of nitrate (NO<sub>3</sub><sup>−</sup>) consumption in Southern Ocean surface waters in the past. During nitrate uptake, phytoplankton preferentially consume <sup>14</sup>N relative to <sup>15</sup>N, resulting in a correlation between the δ<sup>15</sup>N of sinking organic matter and the fraction of the nitrate supply that is consumed in the surface ocean, where δ<sup>15</sup>N = [(<sup>15</sup>N/<sup>14</sup>N)<sub>sample</sub>/(<sup>15</sup>N/<sup>14</sup>N)<sub>air</sub>] − 1. The early application of this correlation was with bulk sedimentary N (10). However, bulk sedimentary δ<sup>15</sup>N can be biased due to diagenetic alteration and contamination by foreign N input, with evidence for major artifacts from these processes in sediment records from both low- and high-latitude sites (11, 12). The δ<sup>15</sup>N of organic matter bound within diatom and foraminifera microfossils avoids these issues and has been applied to reconstruct the nitrate consumption in the AZ and SAZ of the Southern Ocean, respectively (12, 13).

To complement isotopic studies of planktonic microfossil-bound N, we have pursued the N isotopic composition of organic matter bound within the carbonate skeleton of deep-sea scleractinian corals (14). Relative to the sedimentary microfossil-based δ<sup>15</sup>N records, deep-sea corals have the advantages that (i) they feed on organic matter that derives from the sinking flux out of the surface ocean, the δ<sup>15</sup>N of which is forced by mass balance to covary with the degree of nitrate consumption in surface waters (14); (ii) they

## Significance

The concentration of atmospheric carbon dioxide (pCO<sub>2</sub>) varies by 80–100 ppm on glacial–interglacial timescales, with lower pCO<sub>2</sub> during the ice ages. In the modern Southern Ocean, the surface nutrients are not fully consumed by phytoplankton, resulting in leakage of deeply sequestered CO<sub>2</sub> to the atmosphere. It has been suggested that more complete nutrient consumption in the Southern Ocean would have caused the lower pCO<sub>2</sub> during the ice ages. Here, we provide the most spatially comprehensive evidence to date in support of the proposal that the entire Southern Ocean was nutrient-depleted during the last ice age relative to modern conditions. These data are consistent with the hypothesis that Southern Ocean changes contributed to the lower atmospheric pCO<sub>2</sub> of the ice ages.

Author contributions: X.T.W., D.M.S., M.G.P., and G.H.H. designed research; X.T.W., D.M.S., and M.G.P. performed research; X.T.W., J.F.A., L.F.R., S.K.H., A.S.S., A.M.-G., and T.C. contributed new reagents/analytic tools; X.T.W. and J.C. analyzed data; and X.T.W. and D.M.S. wrote the paper.

The authors declare no conflict of interest.

This article is a PNAS Direct Submission.

<sup>1</sup>Present address: Division of Geological and Planetary Sciences, California Institute of Technology, Pasadena, CA 91125.

<sup>2</sup>To whom correspondence should be addressed. Email: xingchen@caltech.edu.

This article contains supporting information online at [www.pnas.org/lookup/suppl/doi:10.1073/pnas.1615718114/-DCSupplemental](http://www.pnas.org/lookup/suppl/doi:10.1073/pnas.1615718114/-DCSupplemental).

can be precisely dated with uranium–thorium (U–Th) and radiocarbon methods, with each coral being an independent constraint on past conditions; and (iii) they are found in both the SAZ and AZ and thus can provide a complete picture of the Southern Ocean from a single fossil type, down to the species level. The >250 fossil corals used in this study were collected from the Drake Passage (DP), with collection sites in both the AZ and SAZ, and from the SAZ south of Tasmania (Fig. 1). All of the corals used in this study are of the solitary species *Desmophyllum dianthus*. The corals were dated by radiocarbon, with ~50 of them also dated using U–Th techniques (Fig. 2). Prior work dating these corals by both approaches provides a basis for the radiocarbon reservoir age correction (15, 16). The five coral sites in the DP can be separated into an SAZ group (Burwood Bank and Cape Horn, to the north of the Subantarctic Front) and an AZ group (Sars, Interim, and Shackleton Fracture Zone, to the south of the Subantarctic Front, Fig. 1 and Fig. S1).

## Results and Discussion

Our coral sites cover a wide range of surface nitrate concentration ( $[\text{NO}_3^-]$ ), from >20  $\mu\text{M}$  in the DP AZ, to ~15  $\mu\text{M}$  in the DP SAZ, to ~3  $\mu\text{M}$  in the Tasmanian SAZ (Fig. 1). Our late Holocene (0–5 kyr) average coral  $\delta^{15}\text{N}$  in the Tasmanian SAZ ( $10.34 \pm 0.99\text{‰}$ ,  $1\sigma$ ,  $n = 37$ ) is higher than that of the DP SAZ ( $8.60 \pm 0.95\text{‰}$ ,  $1\sigma$ ,  $n = 26$ ) and AZ ( $9.01 \pm 1.07\text{‰}$ ,  $1\sigma$ ,  $n = 16$ ), with the DP AZ and SAZ coral  $\delta^{15}\text{N}$  indistinguishable from one another. These values are consistent with expectations based on the Rayleigh model, given the conditions in these regions (SI Text).

The  $\delta^{15}\text{N}$  range in corals of similar ages (Fig. 2) is far greater than the analytical uncertainty [ $1\text{ SD} = 0.2\text{‰}$  (17, 18)]. Complementing this interspecimen variability, analyses from individual coral septa along the growth direction show  $\delta^{15}\text{N}$  variation of 1–2‰ on what would represent decadal timescales (Fig. S2). Such interspecimen and intraspecimen  $\delta^{15}\text{N}$  variation may record region-wide changes in the  $\delta^{15}\text{N}$  of N export, which would be of interest. Alternatively, they may reflect biological (e.g., ontogenetic) variability and/or may result from short timescale changes in deep-particle transport that alter the  $\delta^{15}\text{N}$  of the food supply to the corals. Measurements of recent corals at individual sites suggest  $\delta^{15}\text{N}$  variation of as much as 2‰ in coral carbonate-bound N (e.g., as a function of depth) (14), raising the possibility that this degree of variation is inherent to the proxy, although decadal variation in the regional  $\delta^{15}\text{N}$  of N export may

also be contributing to the range in recent coral  $\delta^{15}\text{N}$  at those sites. Among the Southern Ocean corals studied here (Fig. S2) and others that have been investigated (14), there is no shared trend in  $\delta^{15}\text{N}$  through individual septa. Thus, the  $\delta^{15}\text{N}$  variability both within septa and across specimens is best explained by environmental variability, as opposed to an ontogenetic effect, but this does not allow us to distinguish between regional change in sinking N  $\delta^{15}\text{N}$  (the signal of interest) and local deep-particle dynamics. Further ground-truthing will be required to assess the significance of such short timescale variation in coral  $\delta^{15}\text{N}$ , which we avoid interpreting here. However, it is worth noting that there may be changes in interspecimen  $\delta^{15}\text{N}$  variability through the records, for example, greater variability between 15 and 13 kyr; if confirmed, this may yield important insights into past biogeochemical and environmental conditions. Although the inherent high temporal resolution of deep-sea corals raises their potential for studying high-frequency marine N cycle dynamics in the past, it currently complicates the identification of modest millennial-scale changes. We focus here on the large-scale, long-term trends over the past 40 kyr, which, due to the large number of corals analyzed, emerge despite short-term variability. Monte Carlo and Kalman filter methods are used that incorporate all characterized uncertainties (Fig. 2, Datasets S1 and S2, and Materials and Methods).

**Antarctic Zone.** In the AZ of the Southern Ocean, diatom-bound  $\delta^{15}\text{N}$  records generally indicate more complete nitrate consumption during the last glacial period, but the records vary among cores (8), with an opposite change in the Pacific and Atlantic sectors of the AZ (19), and there are concerns of strong effects from diatom species differences (20). Average coral  $\delta^{15}\text{N}$  is 4–5‰ higher during the Last Glacial Maximum (LGM) than the late Holocene (Fig. 2), consistent with a recent diatom-bound  $\delta^{15}\text{N}$  record from the Pacific AZ near the Antarctic Polar Front (Figs. 1 and 3), where diatom species changes are minor (13). Using the Rayleigh model, we convert the  $\delta^{15}\text{N}$  records to the degree of summertime nitrate consumption (the percentage of the wintertime surface nitrate that is consumed over the summer productive period; SI Text). Both records indicate that the surface nitrate consumption was >90%. Assuming no change in the  $[\text{NO}_3^-]$  or  $\delta^{15}\text{N}$  of underlying Circumpolar Deep Water (which is justified by the observation that the modern values in Circumpolar Deep Water are close to the whole-ocean averages), we calculate a summertime surface  $[\text{NO}_3^-]$  of <5  $\mu\text{M}$  in the LGM Antarctic (SI Text and Fig. S3). The constriction of the DP causes the AZ in that

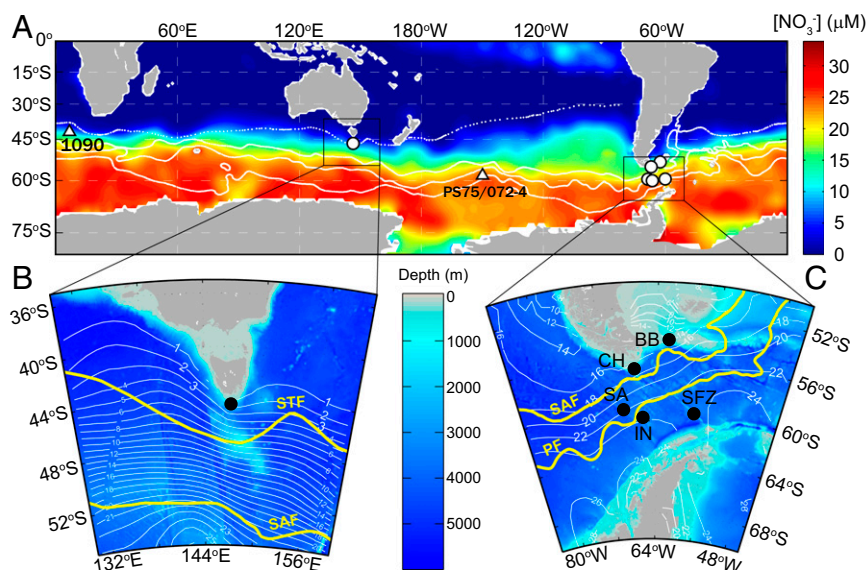


**Fig. 1.** Deep-sea coral sites relative to surface nitrate concentration, ocean fronts, and bathymetry. (A) Southern hemisphere map showing climatological austral summer (December, January, and February) surface nitrate concentration (color scale), fossil coral sites (open, black-rimmed circles), and ocean fronts [white dotted lines, from north to south: Subtropical Front (STF), Subantarctic Front (SAF), Antarctic Polar Front (APF), and Southern Antarctic Circumpolar Current Front (SACCF)]. Shown as open triangles are the locations of two published sediment-based fossil  $\delta^{15}\text{N}$  records: foraminifera-bound  $\delta^{15}\text{N}$  at ODP Site 1090 (12) and diatom-bound  $\delta^{15}\text{N}$  at PS75/072-4 (13). (B) Bathymetric map (color scale) centered on Tasmania showing the deep-sea coral sites (overlapping black circles), austral summer surface nitrate concentration (white contours, in units of micromolar concentration), and the Subtropical and Subantarctic Fronts (yellow lines). (C) As in B but centered on DP and showing its deep-sea coral sites (BB, Burwood Bank; CH, Cape Horn; IN, Interim; SA, Sars; SFZ, Shackleton Fracture Zone).

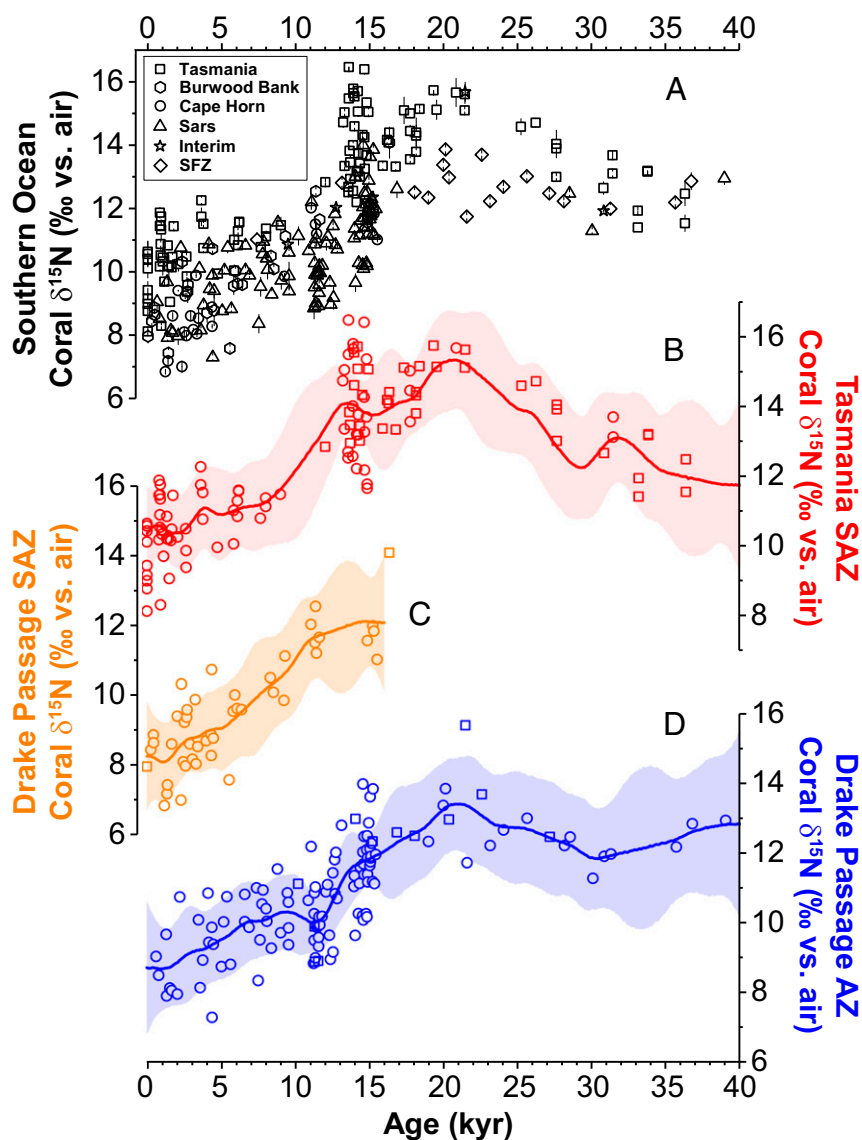


**Fig. 2.** Nitrogen isotopes of Southern Ocean deep-sea corals. (A) All Southern Ocean corals in this study, with the error bars representing analytical precision ( $1\sigma$ ) calculated from two to three replicates of the same subsample from each coral septum; and (B–D) Southern Ocean corals grouped into the Tasmanian SAZ (B) and the DP SAZ (C) and DP AZ (D). In B–D, squares indicate corals with U–Th ages, whereas circles denote corals with radiocarbon ages corrected for the reservoir effect. The mean  $\delta^{15}\text{N}$  histories (bold lines) with error envelopes ( $2\sigma$ ; 95% confidence interval) are simulated with Monte Carlo and Kalman filter methods (Materials and Methods).

region to integrate conditions across most of the latitude range of the AZ in other sectors. Thus, the coral  $\delta^{15}\text{N}$  data provide the strongest evidence to date that the ice age increase in nitrate consumption did not apply solely to sites near the Antarctic Polar Front but rather applied to the full latitude range of the AZ.

**Subantarctic Zone.** In the Tasmanian SAZ record (Fig. 2), the average coral  $\delta^{15}\text{N}$  is 4–5‰ higher during the LGM than the late Holocene, an observation consistent with a foraminifera-bound  $\delta^{15}\text{N}$  record in the Atlantic SAZ (Fig. 3) (12). The Tasmania SAZ coral  $\delta^{15}\text{N}$  record is further corroborated by the coral  $\delta^{15}\text{N}$  compilation from the DP SAZ. In the DP SAZ, no *D. dianthus* older than ~17 kyr were found (21). Nevertheless, coral  $\delta^{15}\text{N}$  also shows a 3.5–4.0‰ decrease from ~15 kyr to the late Holocene (Fig. 2). In sum, the SAZ deep-sea coral  $\delta^{15}\text{N}$  data greatly strengthen the N isotopic evidence for more complete nitrate consumption in the ice age SAZ. Combining these results with those from the AZ, both of the major zones of the Southern Ocean were characterized by more complete nitrate consumption during the last ice age.

Questions exist regarding particle dynamics in the Southern Ocean and specifically the role that circulation may play in the  $\delta^{15}\text{N}$  distribution of deep suspended particles, and this is a concern for paleoceanographic applications of Southern Ocean

deep-sea corals. It would seem plausible that deep-sea particle could be exchanged between the AZ and SAZ, leading to an erroneous interpretation from deep-sea corals regarding nutrient conditions in their region of growth; for example, the SAZ coral  $\delta^{15}\text{N}$  might be argued to respond to AZ nutrient conditions. A range of observations and considerations argues against the dominance of such an effect for the last 40 kyr. First, the ~2‰ higher  $\delta^{15}\text{N}$  of modern corals in the Tasmanian SAZ relative to the DP is consistent with local sinking particles dominating the food source to corals in each region (Fig. S4). Given the evidence for low productivity in the AZ during ice ages (9), contamination of the SAZ by AZ particles would be even less likely during the LGM, and the circulation of the Southern Ocean is inconsistent with SAZ particles substantially influencing the AZ. Second, the Tasmanian SAZ and DP AZ coral  $\delta^{15}\text{N}$  records have coherent differences (Fig. 2B vs. Fig. 2D) that argue against the same history of change being recorded by both regions. Third, the Tasmanian corals are from the northern margin of the SAZ, quite distant from the AZ (Fig. 1), such that most deep particles from the AZ would be decomposed before reaching this far north. Fourth, the deep-sea coral  $\delta^{15}\text{N}$  records are remarkably consistent with both AZ diatom  $\delta^{15}\text{N}$  and SAZ foraminifera  $\delta^{15}\text{N}$  (Fig. 3), and these microfossil-forming plankton are not sensitive to

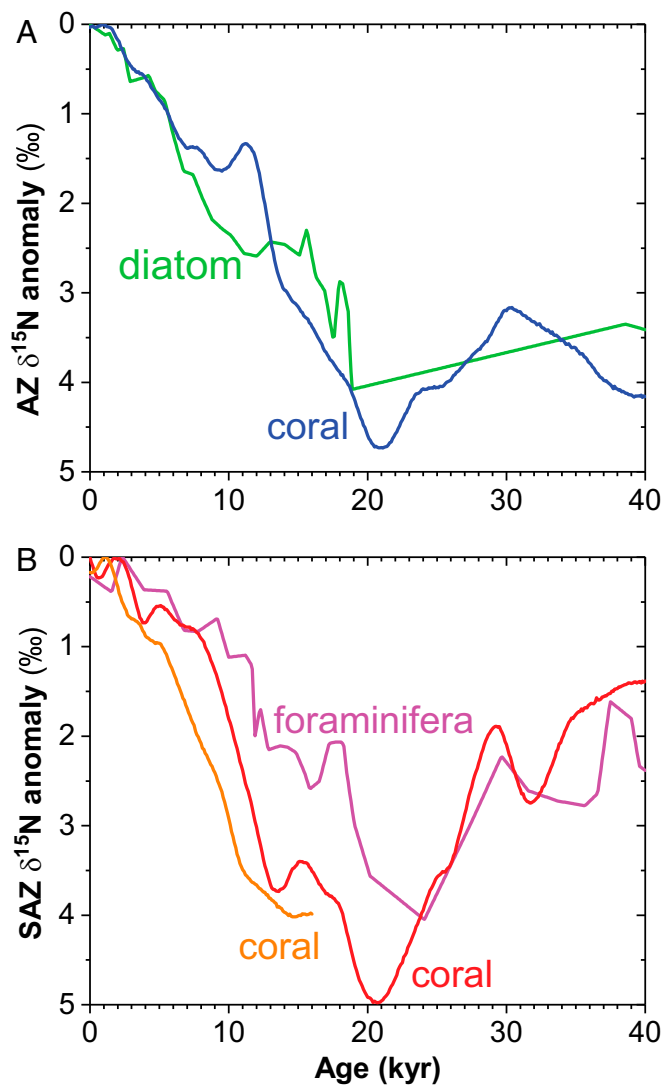


**Fig. 3.** Comparison of coral  $\delta^{15}\text{N}$  records with planktonic microfossil  $\delta^{15}\text{N}$  records from sediment cores, with the  $\delta^{15}\text{N}$  anomaly calculated by subtracting the modern or core-top  $\delta^{15}\text{N}$  values from each record. (A) Comparison of the DP AZ coral mean  $\delta^{15}\text{N}$  record with the P575/072-4 AZ diatom  $\delta^{15}\text{N}$  record (13) and (B) comparison of the SAZ coral mean  $\delta^{15}\text{N}$  records with the ODP Site 1090 SAZ foraminifera  $\delta^{15}\text{N}$  record (12).

deep suspended particle  $\delta^{15}\text{N}$ . Southern Ocean N cycling and the controls on the  $\delta^{15}\text{N}$  of deep suspended particles and deep-sea corals have not been adequately investigated to preclude as-yet-unrecognized complications. Nevertheless, we believe that our interpretation of more complete nitrate consumption across the Southern Ocean during the last ice age is robust.

The SAZ sits downstream of the AZ in the large-scale overturning circulation and today receives a significant fraction of its nitrate from the AZ mixed layer. Because the surface  $[\text{NO}_3^-]$  during the LGM was much lower than today in the AZ, the contribution of the AZ surface to nitrate in the SAZ thermocline and surface mixed layer was lower during the LGM. We simulate this effect with a mixing model (Fig. S5 and SI Text), using the reconstructed changes in AZ  $[\text{NO}_3^-]$  over the last 40 kyr (Fig. S3). The mixing model also indicates that the  $\delta^{15}\text{N}$  of the gross nitrate supply to the SAZ would have varied in response to changes in AZ nitrate concentration and  $\delta^{15}\text{N}$  (Fig. S5). The  $\delta^{15}\text{N}$  of the nitrate supply to the SAZ is calculated to have been similar during the LGM and in the late Holocene,

but with a deglacial maximum ( $\sim 1.5\text{‰}$  higher than the LGM and late Holocene values) (Fig. S6). The estimated rate and  $\delta^{15}\text{N}$  of nitrate supply to the SAZ are combined with the coral  $\delta^{15}\text{N}$  reconstruction from the SAZ to yield a preliminary calculation of the history of  $[\text{NO}_3^-]$  in the SAZ summer mixed layer (Fig. S3B). As with the AZ, during the LGM, the SAZ surface  $[\text{NO}_3^-]$  was  $< 5 \mu\text{M}$  (Fig. S3B). We caution that our quantitative reconstruction of ice age surface  $[\text{NO}_3^-]$  has uncertainties that are poorly characterized. In particular, the SAZ reconstruction relies on changes in nitrate supply that derive from the mixing model, in which the water exchange terms are poorly known today and could also have changed as a function of climate. Numerical modeling frameworks calibrated with modern data have great potential to improve the reconstructions.

To explain lower ice age  $p\text{CO}_2$ , a higher degree of nitrate consumption during ice ages has been proposed for both the AZ and the SAZ (4, 22–24). Our coral  $\delta^{15}\text{N}$  data provide evidence in support of these hypotheses. Remarkably, although the degree of nitrate consumption was higher in both of these regions during the last ice age, the AZ is reconstructed to have hosted much lower biological productivity than during the Holocene, whereas the SAZ hosted higher productivity (Fig. 4) (5, 9). This has led to the interpretation of a circulation-driven ice age reduction in nitrate supply as the ultimate driver of the AZ nitrate consumption change (13), whereas ice age iron fertilization best explains the nitrate consumption increase in the SAZ (Fig. 4D) (12). Given these different mechanisms for changes in surface nitrate, one would not expect identical histories for nitrate consumption in the two regions. Indeed, there are distinctions in the coral  $\delta^{15}\text{N}$  records from the AZ and SAZ both within the last ice age and since the end of the ice age. Below, we focus on the latter.

**Deglacial Changes Across the Southern Ocean.** Combined with the foraminifera and diatom  $\delta^{15}\text{N}$  records (12, 13), our coral  $\delta^{15}\text{N}$  data allow us to compare the deglacial changes in the Southern Ocean  $[\text{NO}_3^-]$  with other relevant environmental changes (Fig. 4). In the AZ,  $[\text{NO}_3^-]$  rose from the LGM to  $\sim 12$  kyr, suggesting that the AZ contributed to the deglacial rise in atmospheric  $p\text{CO}_2$ . Export production in the AZ rose during the same period, consistent with the previous suggestion of a deglacial rise in Southern Ocean overturning (10, 13). Interestingly,  $[\text{NO}_3^-]$  in the AZ continued to increase throughout the Holocene. This feature suggests a rise in the Southern Ocean overturning in the Holocene that may have contributed to the rise in atmospheric  $p\text{CO}_2$  since 8 kyr (25).

In the SAZ, both the coral and foraminifera  $\delta^{15}\text{N}$  records suggest that there were two episodes of deglacial rise in surface  $[\text{NO}_3^-]$  (Figs. 3 and 4). Decreasing iron flux can explain the early to middeglacial increase in  $[\text{NO}_3^-]$ , consistent with ice age iron fertilization in the SAZ (12, 23). However, the second episode of increase in  $[\text{NO}_3^-]$  during the later deglaciation and early Holocene cannot be explained solely by a change in the iron flux, which was low and relatively stable during this period (Fig. 4D). In the iron-limited Southern Ocean, nitrate consumption is widely thought to be modulated by the ratio of rates of iron and nitrate supply (26). Without significant change in the atmospheric iron flux during the late deglaciation and early Holocene, the second episode of deglacial rise in the SAZ  $[\text{NO}_3^-]$  is consistent with an increasing supply of nitrate from the AZ into the SAZ, an expected consequence of the reconstructed rise in AZ surface  $[\text{NO}_3^-]$ . A complication for the deglaciation is that frontal migration likely also changed the  $[\text{NO}_3^-]$  field, shifting lower  $[\text{NO}_3^-]$  poleward. This may have countered the deglacial rise in Southern Ocean surface  $[\text{NO}_3^-]$ , contributing to its apparently gradual nature.

## Conclusion

From this first application of deep-sea coral  $\delta^{15}\text{N}$ , we reconstruct an ice age Southern Ocean without the high  $[\text{NO}_3^-]$  or the strong

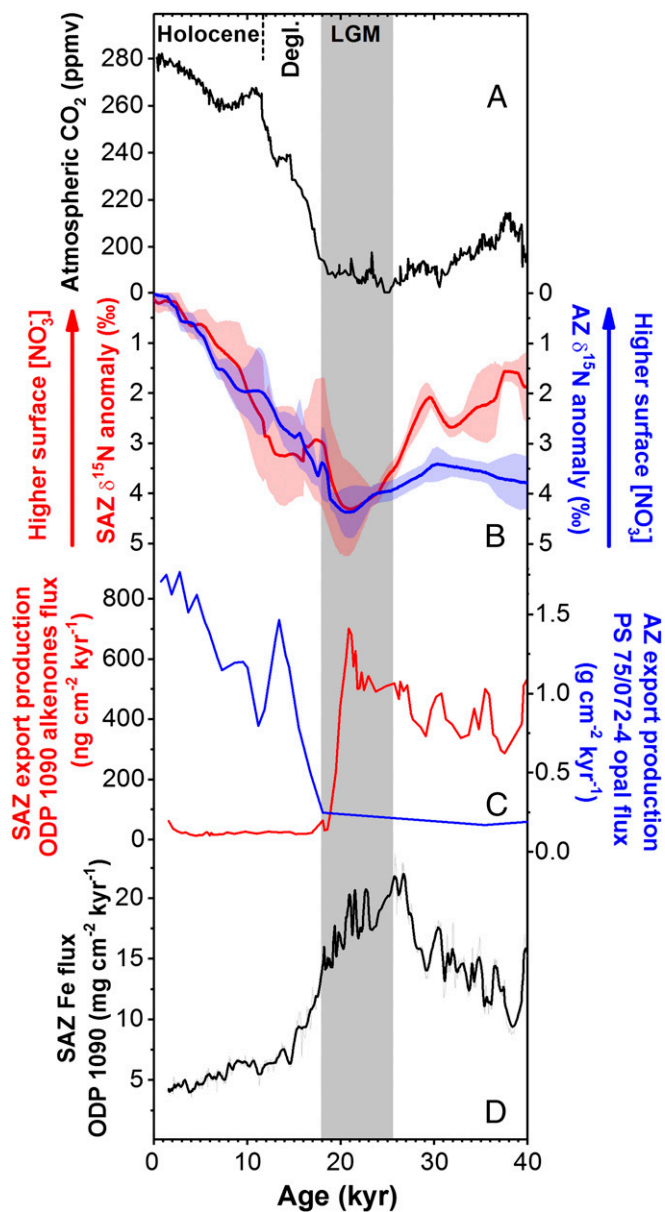


**Fig. 4.** Comparison of Southern Ocean biogeochemical changes and the history of atmospheric  $\text{CO}_2$  concentration over the past 40 kyr. (A) Atmospheric  $\text{CO}_2$  (35, 36); (B) average AZ and SAZ  $\delta^{15}\text{N}$  changes from coral, diatom, and foraminifera records in Fig. 3, with the shading showing  $\pm 1\sigma$  based on all records; (C) SAZ and AZ export productivity (12, 13); and (D) Southern Ocean dust [iron (Fe)] flux as recorded in the Atlantic SAZ (12).

north–south  $[\text{NO}_3^-]$  gradient that characterizes the region today. The picture that arises is of an ice age Southern Ocean state radically different from the modern, in which the two major zones (the Antarctic and the Subantarctic) receive most of their nitrate from below and consume almost all of it in the summertime surface mixed layer. This argues strongly for a central role of the biogeochemistry of the Southern Ocean in lowering ice age  $p\text{CO}_2$ .

At the same time, the data appear to indicate that the Southern Ocean  $[\text{NO}_3^-]$  rise of the last deglaciation was incomplete, with additional change through the Holocene (Fig. 4B). Given model calculations of the  $p\text{CO}_2$  decline achieved by different Southern Ocean changes (22), the incomplete nature of Southern Ocean biogeochemical change across the early deglaciation suggests that it

was not the sole driver of the early deglacial  $p\text{CO}_2$  rise. The warming-driven decline in the solubility of  $\text{CO}_2$  in the deep ocean, which appears to have occurred early in the deglaciation (27), may thus have been critical in the first deglacial increase in atmospheric  $p\text{CO}_2$ . There is as-yet no evidence for such a lag of Southern Ocean biogeochemical change relative to Southern Ocean climate for prior glacial terminations (12, 13), but addressing this question requires better age constraints, such as might arise from U–Th dating of deep-sea corals from those terminations.

## Materials and Methods

**Deep-Sea Coral Collection.** Deep-sea fossil corals in the DP were collected by dredge or trawl (21), whereas a deep submergence vehicle was used to collect coral samples from the Tasmanian seamounts (28). Detailed information on all coral samples used in this study is given in refs. 15 and 16.

**Radiocarbon Dating.** From each individual coral, a small (~40 mg) piece was cut and physically abraded using a Dremel tool to remove the Fe–Mn crust. Samples were then cleaned and radiocarbon dated with methods detailed in refs. 29 and 30. The calendar age was calculated from the measured radiocarbon content and an estimated reservoir age (15, 16, 21, 28).

**Uranium–Thorium Dating.** A subset of the corals used in this study (~20%; shown as squares in Fig. 2) was also subjected to the U–Th dating method (15, 16). Briefly, a piece (0.3–1 g) of coral was cut and physically cleaned using a Dremel tool and then chemically cleaned following ref. 31. After cleaning, the coral was dissolved in nitric acid to dissolve the sample and a mixed  $^{236}\text{U}$ – $^{229}\text{Th}$  spike added. The U and Th were separated, purified, and measured separately by multicollector inductively coupled plasma mass spectrometer. All U–Th ages used in this study have been published in refs. 15 and 16.

**Age Model.** The final age model for the three coral  $\delta^{15}\text{N}$  records is composed of two parts (Fig. 2). Whenever the U–Th ages are available, they are used in the final age model as the calendar age. When U–Th ages are not available, the calendar age is calculated from the radiocarbon age after correction for the water mass radiocarbon content (i.e., reservoir effect), based on the reservoir ages of coral samples for which both U–Th ages and radiocarbon ages have been measured (15, 16).

**Nitrogen Isotope Analysis.** The protocol for nitrogen isotope analysis was detailed in refs. 14, 32, and 33. Briefly, 5–10 mg of mechanically cleaned coral septum is ground into coarse powder (with a grain size of a few hundred micrometers) and sonicated for 5 min in 2% (wt/vol) sodium polyphosphate in a 15-mL polypropylene centrifuge tube to remove any detrital material attached to the sample. The sample is rinsed (by filling, centrifugation, and decanting) three times with deionized water (DIW) and reductively cleaned using sodium bicarbonate-buffered dithionite–citrate reagent to remove any metal coatings. After three to four rinses with DIW, the sample is cleaned for 24 h using 10–15% sodium hypochlorite to remove external organic N contamination and again rinsed three to four times with DIW. After cleaning, the sample is dried in an oven at 60 °C and dissolved in 4 M hydrochloric acid. The released organic matter is oxidized to nitrate using a basic potassium persulfate solution. The resulting dissolved nitrate is converted bacterially into nitrous oxide, which is measured for its  $\delta^{15}\text{N}$  by automated extraction and gas chromatography–isotope ratio mass spectrometry (34). Amino acid standards with known  $\delta^{15}\text{N}$  (USGS 40 and 41) are included in each batch of samples to correct for the blank associated with persulfate reagent, which is less than 2% of the total N content in an oxidized sample. Each ground sample was processed in duplicate through the entire cleaning and analysis protocol. An in-house coral standard was used in each batch of analysis as quality control and yields a long-term precision better than 0.2‰ ( $1\sigma$ ) (32).

To evaluate the  $\delta^{15}\text{N}$  variation in single septa, multiple samples were cut out along the growth direction of each single septum and analyzed for  $\delta^{15}\text{N}$  using the above method. The results for these samples are shown in Fig. S2 and discussed in *Results and Discussion*.

**Mann–Whitney U Test.** To evaluate the statistical significance of the coral  $\delta^{15}\text{N}$  datasets, Mann–Whitney U tests were performed on the  $\delta^{15}\text{N}$  time series for each 5-kyr bin (except for 20–40 kyr; Fig. S4).

**N Isotopes vs. N Content in Corals.** To evaluate the effect of N content in driving the observed trend in our coral  $\delta^{15}\text{N}$ , we performed a correlation

analysis and showed that the coral  $\delta^{15}\text{N}$  variation cannot be explained by the changes in N content in any of the three records (Fig. S7).

**Monte Carlo and Kalman Filter Simulation.** Monte Carlo simulation and Kalman smoother were combined to obtain a best estimate of the average  $\delta^{15}\text{N}$  time series on a regular time grid and its corresponding confidence interval. First,  $M$  synthetic time series of  $\delta^{15}\text{N}$  were generated by adding errors to both age and  $\delta^{15}\text{N}$  measurements. The errors are normally distributed random numbers with zero mean and specified SDs ( $\sigma$ ). The SDs for the measured age were assigned to be 500 y (typically larger than the actual measured age uncertainty), and the SDs for the measured  $\delta^{15}\text{N}$  are from the actual measurement errors (including both analytical error and variation in single coral septa). Then, for each one of the  $M$  synthetic time series of  $\delta^{15}\text{N}$ , a Kalman smoother was applied to obtain the best estimate for  $\delta^{15}\text{N}$  and its SD on a regular time grid. For each of the best estimates,  $N$  time series were

generated to represent the probability distribution of this best estimate (by adding normally distributed random numbers with zero mean and SDs to the time series). Thus, outcome was  $M \times N$   $\delta^{15}\text{N}$  series on a regular grid. At each time, the best estimate for  $\delta^{15}\text{N}$  was obtained from the average of the  $M \times N$   $\delta^{15}\text{N}$  series, and the confidence interval was obtained from the  $\sigma$  of the  $M \times N$   $\delta^{15}\text{N}$  series [plotted as 95% confidence interval ( $2\sigma$ ) in Fig. 2].

**ACKNOWLEDGMENTS.** We thank two anonymous reviewers for their constructive comments. This work was supported by National Science Foundation Grants OCE-1234664 (to M.G.P. and D.M.S.), PLR-1401489 (to D.M.S.), and OCE-1503129 (to J.F.A.), the Charlotte Elizabeth Procter Fellowship of the Graduate School at Princeton University (to X.T.W.), the Grand Challenges Program of Princeton University (D.M.S.), European Research Council Grant 278705 (to L.F.R.), and Natural Environmental Research Council Grant NE/N003861/1 (to L.F.R.).

- Sarmiento JL, Toggweiler JR (1984) A new model for the role of the oceans in determining atmospheric  $p\text{CO}_2$ . *Nature* 308:621–624.
- Martin JH, Gordon RM, Fitzwater SE (1990) Iron in Antarctic waters. *Nature* 345(6271):156–158.
- Mitchell BG, Brody EA, Holm-Hansen O, McClain C, Bishop J (1991) Light limitation of phytoplankton biomass and macronutrient utilization in the Southern Ocean. *Limnol Oceanogr* 36(8):1662–1677.
- Sigman DM, Hain MP, Haug GH (2010) The polar ocean and glacial cycles in atmospheric  $\text{CO}_2$  concentration. *Nature* 466(7302):47–55.
- Kohfeld KE, Le Quéré C, Harrison SP, Anderson RF (2005) Role of marine biology in glacial-interglacial  $\text{CO}_2$  cycles. *Science* 308(5718):74–78.
- Neffel A, Oeschger H, Schwander J, Stauffer B, Zumbunn R (1982) Ice core sample measurements give atmospheric  $\text{CO}_2$  content during the past 40,000 yr. *Nature* 295:220–223.
- Ziegler M, Diz P, Hall IR, Zahn R (2013) Millennial-scale changes in atmospheric  $\text{CO}_2$  levels linked to the Southern Ocean carbon isotope gradient and dust flux. *Nat Geosci* 6(6):457–461.
- Robinson RS, Sigman DM (2008) Nitrogen isotopic evidence for a poleward decrease in surface nitrate within the ice age Antarctic. *Quat Sci Rev* 27(9–10):1076–1090.
- Jaccard SL, et al. (2013) Two modes of change in Southern Ocean productivity over the past million years. *Science* 339(6126):1419–1423.
- Francois R, et al. (1997) Contribution of Southern Ocean surface-water stratification to low atmospheric  $\text{CO}_2$  concentrations during the last glacial period. *Nature* 389(6654):929–935.
- Straub M, et al. (2013) Changes in North Atlantic nitrogen fixation controlled by ocean circulation. *Nature* 501(7466):200–203.
- Martínez-García A, et al. (2014) Iron fertilization of the Subantarctic ocean during the last ice age. *Science* 343(6177):1347–1350.
- Studer AS, et al. (2015) Antarctic Zone nutrient conditions during the last two glacial cycles. *Paleoceanography* 30:845–862.
- Wang XT, et al. (2014) Isotopic composition of carbonate-bound organic nitrogen in deep-sea scleractinian corals: A new window into past biogeochemical change. *Earth Planet Sci Lett* 400(C):243–250.
- Burke A, Robinson LF (2012) The Southern Ocean's role in carbon exchange during the last deglaciation. *Science* 335(6068):557–561.
- Hines SKV, Southon JR, Adkins JF (2015) A high-resolution record of Southern Ocean intermediate water radiocarbon over the past 30,000 years. *Earth Planet Sci Lett* 432:46–58.
- Smart SM, et al. (2015) Isotopic evidence for nitrification in the Antarctic winter mixed layer. *Global Biogeochem Cycles* 29(4):427–445.
- DiFiore PJ, et al. (2006) Nitrogen isotope constraints on subantarctic biogeochemistry. *J Geophys Res Oceans* 111:C08016.
- Robinson RS, Brzezinski MA, Beucher CP, Horn MGS, Bedsole P (2014) The changing roles of iron and vertical mixing in regulating nitrogen and silicon cycling in the Southern Ocean over the last glacial cycle. *Paleoceanography* 29:1179–1195.
- Jacot Des Combes H, et al. (2008) Diatom  $\delta^{13}\text{C}$ ,  $\delta^{15}\text{N}$ , and  $\text{C/N}$  since the Last Glacial Maximum in the Southern Ocean: Potential impact of species composition. *Paleoceanography* 23:PA4209.
- Margolin AR, et al. (2014) Temporal and spatial distributions of cold-water corals in the Drake Passage: Insights from the last 35,000 years. *Deep Sea Res Part II Top Stud Oceanogr* 99:237–248.
- Hain MP, Sigman DM, Haug GH (2010) Carbon dioxide effects of Antarctic stratification, North Atlantic Intermediate Water formation, and subantarctic nutrient drawdown during the last ice age: Diagnosis and synthesis in a geochemical box model. *Global Biogeochem Cycles* 24:GB4023.
- Martin JH (1990) Glacial-interglacial  $\text{CO}_2$  change: The iron hypothesis. *Paleoceanography* 5(1):1–13.
- Broecker WS (1982) Glacial to interglacial changes in ocean chemistry. *Prog Oceanogr* 11(2):151–197.
- Moreno PI, Francois JP, Moy CM, Villa-Martínez R (2010) Covariability of the Southern Westerlies and atmospheric  $\text{CO}_2$  during the Holocene. *Geology* 38(8):727–730.
- Lefèvre N, Watson AJ (1999) Modeling the geochemical cycle of iron in the oceans and its impact on atmospheric  $\text{CO}_2$  concentrations. *Global Biogeochem Cycles* 13(3):727–736.
- Stott L, Timmermann A, Thunell R (2007) Southern Hemisphere and deep-sea warming led deglacial atmospheric  $\text{CO}_2$  rise and tropical warming. *Science* 318(5849):435–438.
- Thiagarajan N, et al. (2013) Movement of deep-sea coral populations on climatic timescales. *Paleoceanography* 28(2):227–236.
- Burke A, et al. (2010) Reconnaissance dating: A new radiocarbon method applied to assessing the temporal distribution of Southern Ocean deep-sea corals. *Deep Sea Res Part I Oceanogr Res Pap* 57(11):1510–1520.
- Bush SL, et al. (2013) Simple, rapid, and cost effective: A screening method for  $^{14}\text{C}$  analysis of small carbonate samples. *Radiocarbon* 55(2–3):631–640.
- Cheng H, Adkins J, Edwards RL, Boyle EA (2000) U-Th dating of deep-sea corals. *Geochim Cosmochim Acta* 64(14):2401–2416.
- Wang XT, et al. (2015) Isotopic composition of skeleton-bound organic nitrogen in reef-building symbiotic corals: A new method and proxy evaluation at Bermuda. *Geochim Cosmochim Acta* 148(C):179–190.
- Ren H, et al. (2009) Foraminiferal isotope evidence of reduced nitrogen fixation in the ice age Atlantic Ocean. *Science* 323(5911):244–248.
- Sigman DM, et al. (2001) A bacterial method for the nitrogen isotopic analysis of nitrate in seawater and freshwater. *Anal Chem* 73(17):4145–4153.
- Ahn J, Brook EJ (2014) Siple Dome ice reveals two modes of millennial  $\text{CO}_2$  change during the last ice age. *Nat Commun* 5:3723.
- Lüthi D, et al. (2008) High-resolution carbon dioxide concentration record 650,000–800,000 years before present. *Nature* 453(7193):379–382.
- Altabet MA, Francois R (1994) Sedimentary nitrogen isotopic ratio as a recorder for surface ocean nitrate utilization. *Global Biogeochem Cycles* 8(1):103–116.
- Altabet MA, Francois R (2001) Nitrogen isotope biogeochemistry of the Antarctic Polar Frontal Zone at  $170^\circ\text{W}$ . *Deep Sea Res Part II Top Stud Oceanogr* 48(19–20):4247–4273.
- Lourey MJ, Trull TW (2001) Seasonal nutrient depletion and carbon export in the Subantarctic and Polar Frontal Zones of the Southern Ocean south of Australia. *J Geophys Res Oceans* 106(C12):31463–31487.
- Rafter PA, DiFiore PJ, Sigman DM (2013) Coupled nitrate nitrogen and oxygen isotopes and organic matter remineralization in the Southern and Pacific Oceans. *J Geophys Res Oceans* 118(10):4781–4794.
- Deutsch C, Sigman DM, Thunell RC, Meckler AN, Haug GH (2004) Isotopic constraints on glacial/interglacial changes in the oceanic nitrogen budget. *Global Biogeochem Cycles* 18:GB4012.
- Galbraith ED, et al. (2013) The acceleration of oceanic denitrification during deglacial warming. *Nat Geosci* 6(7):579–584.
- Haug GH, et al. (1998) Glacial/interglacial variations in production and nitrogen fixation in the Cariaco Basin during the last 580 kyr. *Paleoceanography* 13(5):427–432.
- Tyrrill T (1999) The relative influences of nitrogen and phosphorus on oceanic primary production. *Nature* 400(6744):525–531.
- DiFiore PJ, et al. (2010) Poleward decrease in the isotope effect of nitrate assimilation across the Southern Ocean. *Geophys Res Lett* 37:L17601.
- Granger J, Sigman DM, Rohde MM, Maldonado MT, Tortell PD (2010) N and O isotope effects during nitrate assimilation by unicellular prokaryotic and eukaryotic plankton cultures. *Geochim Cosmochim Acta* 74(3):1030–1040.
- Sigman DM, Altabet MA, McCorkle DC, Francois R, Fischer G (2000) The  $\delta^{15}\text{N}$  of nitrate in the Southern Ocean: Nitrogen cycling and circulation in the ocean interior. *J Geophys Res Oceans* 105(C8):19599–19614.
- Palter JB, Sarmiento JL, Gnanadesikan A, Simeon J, Slater RD (2010) Fueling export production: Nutrient return pathways from the deep ocean and their dependence on the Meridional Overturning Circulation. *Biogeochemistry* 7(11):3549–3568.